J Mater Sci: Mater Electron (2008) 19:493–499
DOI 10.1007/s10854-008-9604-6

REVIEW

# Nanoporous ZnO thin films deposited by electrochemical anodization: effect of UV light

**P. K. Basu · N. Saha · S. Maji · H. Saha · Sukumar Basu**

Received: 27 September 2007 / Accepted: 24 January 2008 / Published online: 12 February 2008


**Abstract** Nanoporous ZnO thin films were deposited by electrochemical anodization of high purity Zn at room temperature using Pt counter electrode, calomel reference electrode and oxalic acid as the electrolyte. The crystallinity and the surface morphology were studied by X-ray diffraction (XRD) and Field emission scanning electron microscope (FESEM). The variation in molar concentration of oxalic acid during anodization had significant effect on the crystal size and the pore size particularly in the presence of UV light. An increase in room temperature band gap from 3.25 to 3.87 eV of ZnO film grown in 0.3 M oxalic acid indicates a quantum confinement effect and it was further confirmed by a blue shift of the photoluminescence (PL) spectra. A possible mechanism of the anodization and the photoetching in the presence of UV light of the ZnO film have been suggested.

## 1 Introduction

The rich defect chemistry of ZnO gives rise to a wide range of properties including piezoelectricity and ferroelectricity, wide band gap semiconductivity, room temperature ferromagnetism, huge magneto-optic effect and chemical sensing [1–6]. Due to its thermal and chemical stability, wide band gap (3.37 eV at RT) and large exciton binding energy (60 meV), ZnO is also a promising material for optoelectronics [7–9].

P. K. Basu · N. Saha · S. Maji · H. Saha · S. Basu (✉)
IC Design & Fabrication Centre, Department of Electronics & Telecommunication Engineering, Jadavpur University, Kolkata 700032, India
e-mail: sukumar_basu@yahoo.co.uk

It is realized that nanomaterials have great potential for the technological development almost in each area in near future. The nanomaterials have some novel properties that attract today for fundamental and technological research and development. The dots and wires in the nanoscale range develop the unique electrical and optical properties of materials. Quantum confinement effect due to the change in size and shape of the nanoparticles can modify the energy bands of the semiconductors and insulating materials. A large section of the research groups have devoted their efforts towards the development of nanostructured ZnO, since the reactions at the grain boundaries and a complete depletion of the carriers in the grains can strongly modify the material transport properties of ZnO. With such a wide range of functional properties, ZnO already finds applications in sensors, optoelectronics and catalysis [10–11].

Compact ZnO films can be prepared by many methods, such as sputtering, pulsed laser deposition [12], chemical vapour deposition [13], sol gel process and electrochemical process [14–15]. However, there are only a few reports on the preparation of ZnO thin films with nanoporous structure. During the past decade, templating of colloidal crystals was one of the most attractive methods used to obtain a porous structure [16–17]. Both two- and three-dimensional ordered porous zinc oxide films were fabricated by electrodeposition using three-dimensional polystyrene opal templates and alumina templates [18–19].

The electrochemical route has greater potential to control the dimensionality through variation of electrolyte concentration and applied potential at room temperature and so it allows the precise control of the reaction conditions. In this study, nanocrystalline–nanoporous ZnO films were prepared by electrochemical anodization of Zinc without and with the exposure of UV light. Detailed

characterizations for crystallinity, morphology, grain structure, optical absorption and PL were performed to establish the quality of the nanoporous ZnO thin films.

## 2 Experimental

A properly cleaned high purity Zn (99.9% purity, Aldrich Chemicals, USA) of thickness 0.5 mm was taken as anode and the platinum as cathode. A calomel electrode was employed as the reference electrode. The Zn was anodized in different concentrations (0.3, 0.5 and 1 M) of oxalic acid (99%, MERCK, India) with constant 10 V potentiostatic (Scanning Potentiostat-362, Princeton Applied Research, USA) power supply. The separation between the anode and the cathode was 18 mm. The calomel reference electrode was placed very near to anode with a distance of 5 mm. The anodization was carried out in absence and in the presence of UV light in the pulse mode (Dr. Grobel, UV-Elektronik GmbH UV-LQ 400). With the initiation of anodization the current started decreasing and finally got saturated. The polycrystalline phase, the crystal size, the surface morphology and the pore size of the anodized ZnO films were studied by XRD (Bruker DH Advance) and by FESEM (JEOL, JSM-6700 F). The thickness of the films was measured by a Surface Profilo Meter (Sloan Technology, DEKTAK Surface profilers, Veeco, Version-1.05). PL spectra (Spectra Physics Model-74100) of the grown films were taken. The band gap of the ZnO films was measured by the optical absorption (Shimadzu UV-3101 PC) method. The electrical resistivity of the samples was measured using two point probe configuration and indium ohmic contact.

## 3 Results

### 3.1 X-ray diffraction study

The XRD pattern of ZnO films anodized without and with UV light and at different concentrations of oxalic acid is shown in Fig. 1 displaying the presence of polycrystalline phase with (101) and (110) orientations. The (101) peak of the films grown in the presence of UV light shows higher intensity. The Fig 1a shows the XRD peaks of ZnO thin films anodized in 0.3 M oxalic acid. The intensity of the ZnO (101) peak increases and that of Zn (101) peak reduces for the films grown in the presence of UV. Figure 1b shows the XRD patterns of ZnO thin films anodized in 0.5 M oxalic acid. It is seen that the intensity of both the (101) and (110) peaks increase but the Zn (101) peak reduces for the UV-assisted grown films. The similar effects are observed for the ZnO films anodized in 1 M oxalic acid (Fig. 1c). The increase in intensity of the films grown in presence of UV is mainly due to the crystal growth caused by the enhanced rate of oxidation due to excess hole generation. The crystal sizes of the samples were calculated from the Scherer formula:

$$D = \frac{0.9\lambda}{B\mathrm{Cos}\ \theta}$$

where $\lambda$ is the wavelength of X-ray radiation, $B$ is the value of FWHM and $\theta$ is the diffraction angle. Table 1 presents the crystal size of ZnO films grown at different electrolyte concentrations.

### 3.2 FESEM study

The surface morphology of the ZnO thin films anodized in different concentrations of oxalic acid was studied by FESEM and is shown in Fig. 2. The average crystal size and the pore diameters are shown in Table 1 and it is clear that the UV light during deposition has a great role to play on the crystal size and the porosity of the ZnO thin films. The higher grain size at the higher concentrations of oxalic acid is due to the higher grain growth which was further influenced by the UV light during anodization. FESEM pictures clearly display the phenomena of grain growth.

### 3.3 The Electrical resistivity measurements

The electrical resistivity of the samples was determined by the well known formula

$$\rho = \frac{AR}{l}$$

where $\rho$ is the resistivity of the sample, $A$ is the area of the electrode, $l$ is the thickness of the sample and $R$ is the resistance between the two electrodes. The thickness of the samples was measured with the help of a surface profilometer and the values are shown in Table 2. The resistivity of the samples deposited without and with UV is also shown in Table 2. From the table it is observed that the ZnO thin films grown with UV light exposure have lower thickness and higher resistivity than the films grown without UV light.

### 3.4 Optical absorption

Figure 3 shows the optical absorption spectra of the ZnO thin films anodized in different concentrations of oxalic acid electrolyte (0.3, 0.5 and 1 M) without and with UV light exposure. The optical band gap of the films was determined following Davis and Mott [20] model in the high absorbance region using the relation given below,

$$\alpha h\nu = A\,(h\nu - Eg)^{n}$$

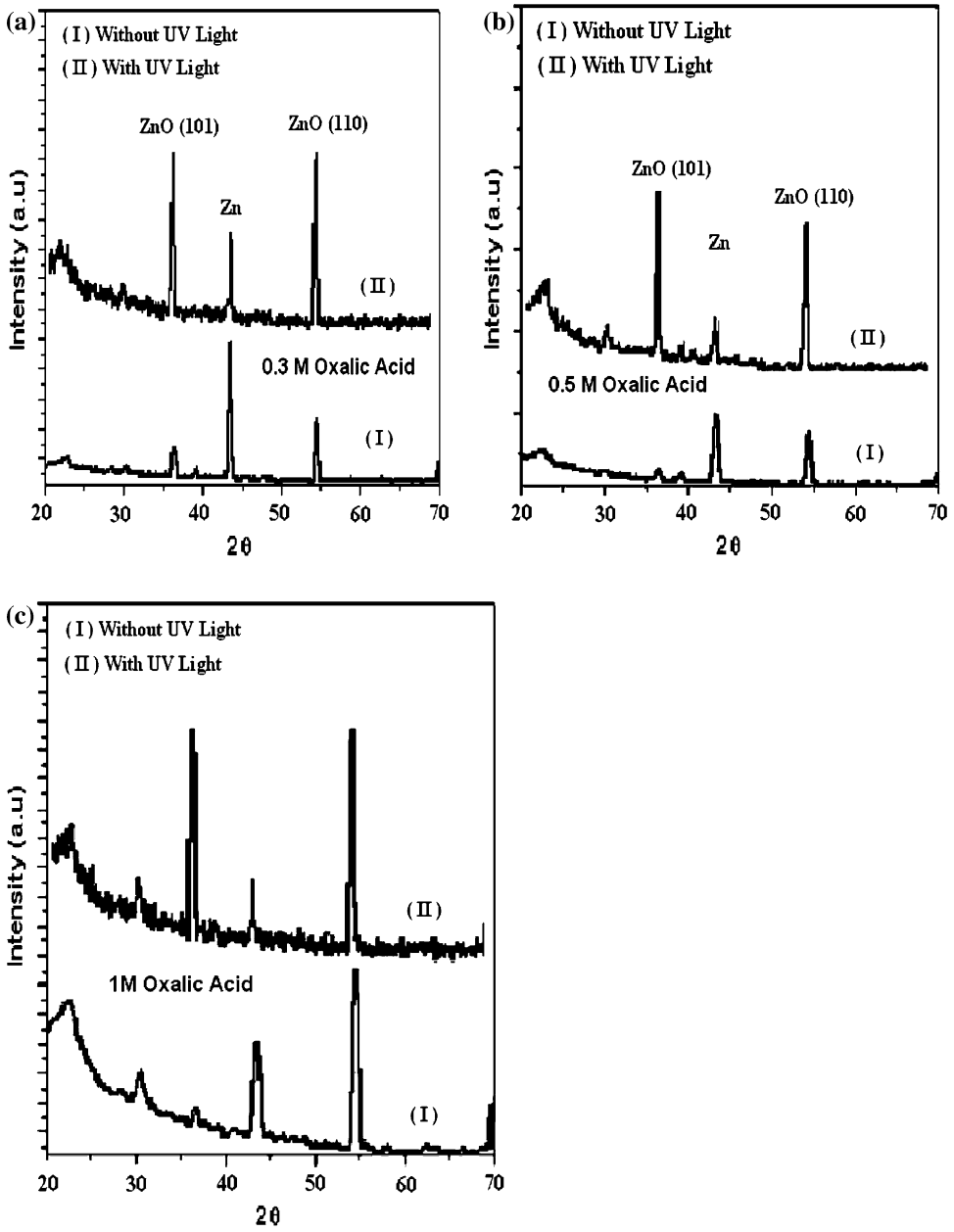


**Fig. 1** XRD pattern of ZnO thin films obtained by anodization of Zn in (**a**) 0.3 M oxalic acid (**b**) 0.5 M oxalic acid and (**c**) 1 M oxalic acid. The crystallinity of UV-assisted grown ZnO thin film is higher than that of the film grown without UV light at all the three oxalic acid concentrations

**Table 1** The effect of UV light during anodization on the crystal size and the pore size

| Concentrations of oxalic acid (M) | Without UV light | | With UV light | |
|---|---|---|---|---|
| | Crystal size (nm) | Pore diameter (nm) | Crystal size (nm) | Pore diameter (nm) |
| 0.3 | 2.41 | 19–35 | 2.67 | 40–45 |
| 0.5 | 3.02 | 45–70 | 3.38 | 50–96 |
| 1 | 5.22 | 70–90 | 8.06 | 135–140 |

where h$\nu$ is the photon energy, $Eg$ is the optical band gap, and A is a constant. For direct transition $n = 1/2$ or 2/3 and $n = 1/2$ was found to be more suitable for ZnO thin films since it gives the best linear curve in the band edge region [21]. The $Eg$ value can be obtained by extrapolating the linear portion of the spectrum to the photon energy axis as is shown in Fig. 3. The optical band gap values obtained are summarized in Table 3.

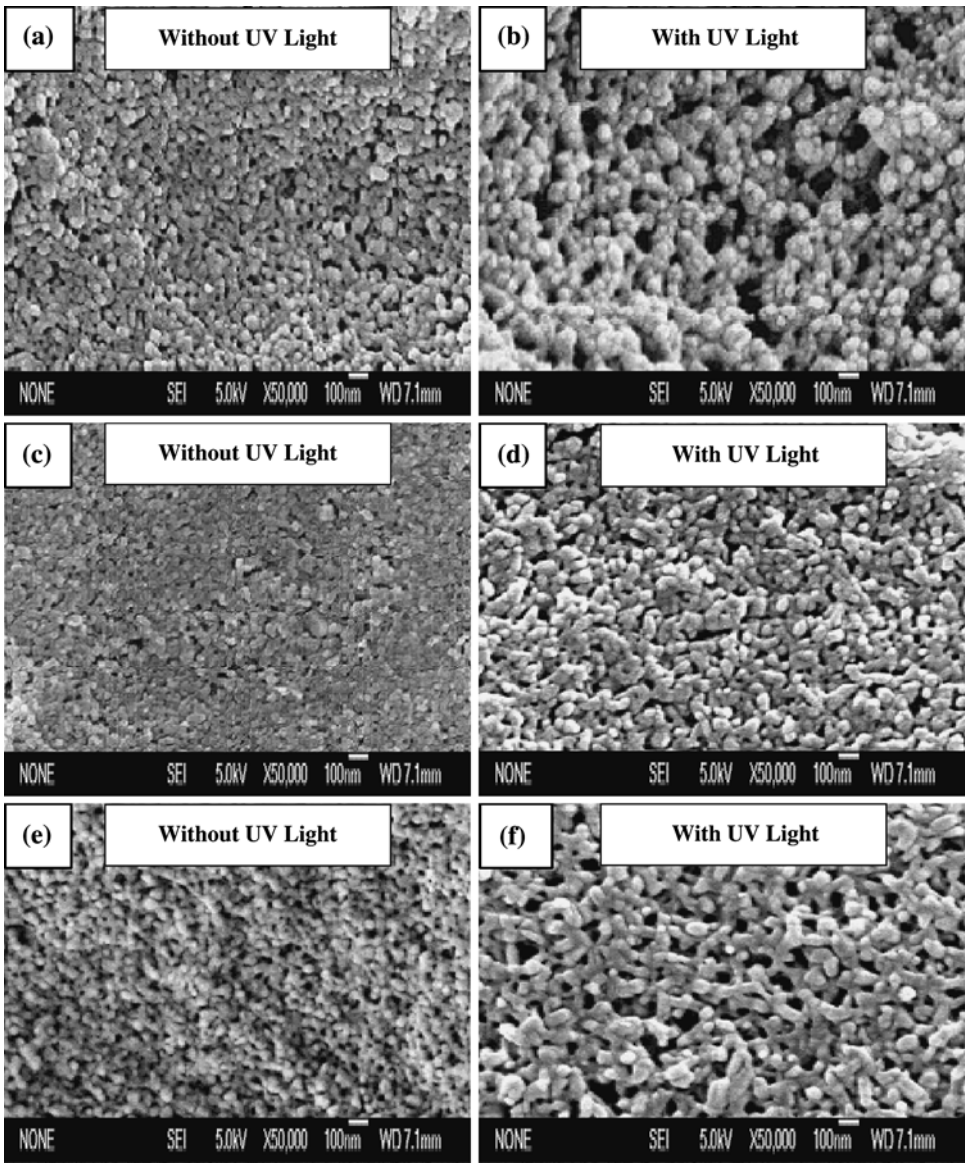


**Fig. 2** (**a**, **b**), (**c**, **d**) and (**e**, **f**) are the FESEM pictures of ZnO thin films obtained by anodization of Zn in 0.3, 0.5 and 1 M oxalic acid without and with the exposure of UV light, respectively. It is observed that the pore size and the grain size of UV assisted grown ZnO thin film are larger than that of the film grown without UV light

**Table 2** Thickness and resistivity of the ZnO thin films grown without and with UV radiation

| Concentrations of oxalic acid (M) | Without UV | | With UV | |
|---|---|---|---|---|
| | Thickness (μm) | Resistivity (Ωm) | Thickness (μm) | Resistivity (Ωm) |
| 0.3 | 8.2 | $3.95 \times 10^6$ | 4.8 | $7.39 \times 10^6$ |
| 0.5 | 16 | $2.81 \times 10^6$ | 6.2 | $6.77 \times 10^6$ |
| 1 | 18.2 | $1.86 \times 10^6$ | 9.2 | $2.33 \times 10^6$ |

The table shows that as the concentrations of the electrolyte are reduced from 0.5 to 0.3 M during deposition of the ZnO film, the optical band gap is blue shifted from 3.23 to 3.87 eV for the samples grown without UV light and 3.24–3.79 eV for the UV-assisted grown samples. This shift in the band gap firmly attests the theory of quantum confinement effect and can be described by the following equation [22–23]:

$$Eg = E_{\text{Bulk}} + \frac{\hbar^2\pi^2}{2R^2}\left(\frac{1}{m_e*} + \frac{1}{m_h*}\right) - 0.248E_{\text{ry}}$$

where $E_g$ is the absorption band gap of nanosemiconductor particles, The bulk band gap $E_{\text{bulk}}$ for ZnO (3.2 eV) at room temperature and the bulk exciton binding energy $E_{\text{ry}}$ (60 meV). The electron and hole effective masses are $m_e* = 0.24\ m_0$ and $m_h* = 2.31\ m_0$ [24]. Additionally, $h$ is

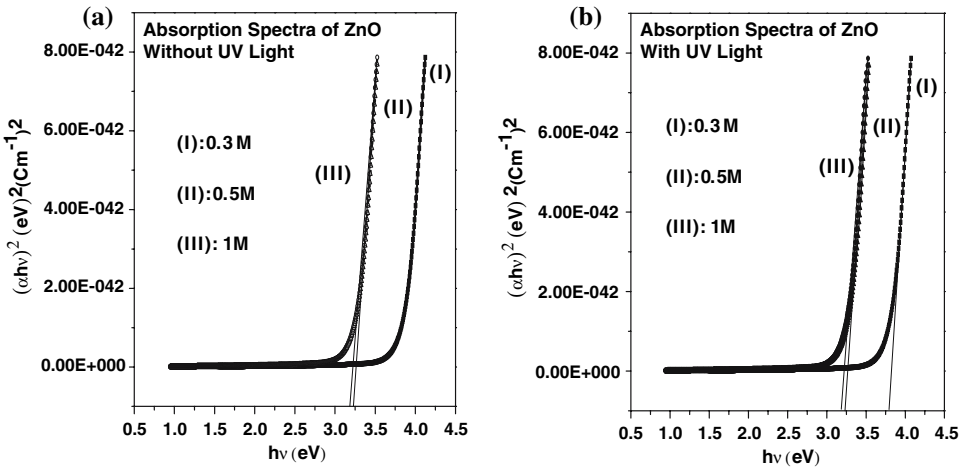


**Fig. 3** Optical absorption spectra of ZnO films obtained by anodization in different concentrations of oxalic acid (**a**) in absences of UV light and (**b**) in the presence of UV light. There is a significant increase in the optical band gap of the film grown in 0.3 M oxalic acid

**Table 3** Optical band gap of the anodic ZnO thin films

| Concentrations of oxalic acid (M) | Optical band gap (eV) | |
|---|---|---|
| | Without UV light | With UV light |
| 0.3 | 3.87 | 3.79 |
| 0.5 | 3.23 | 3.24 |
| 1 | 3.25 | 3.25 |

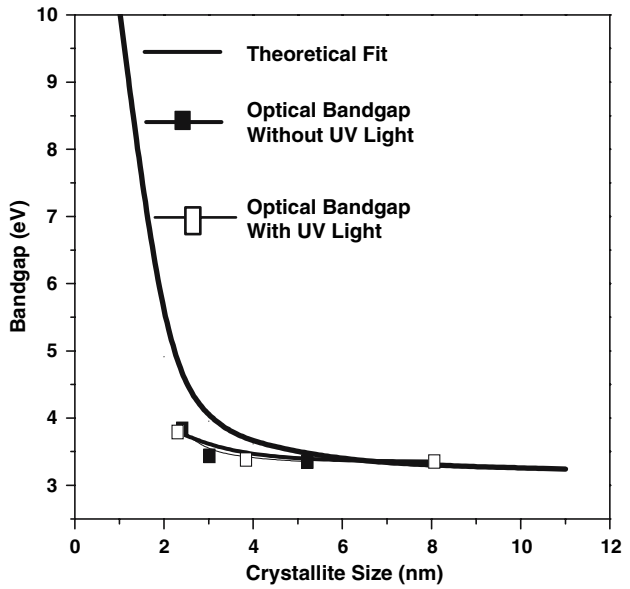


**Fig. 4** Optical band gap versus crystal size plots for the ZnO films grown in absence and in the presence of UV light and the same calculated theoretically

Planck's constant and $R$ is the radius of ZnO nanocrystal. Figure 4 shows a plot of nanocrystal band gap versus the crystal diameter calculated from the above equation. It can be seen that nanocrystal band gap of all the samples measured from the optical absorptions more or less fits the theoretical curve.

### 3.5 Photoluminescence study

Figure 5 shows the room temperature PL spectra of ZnO films deposited in 1, 0.5 and 0.3 M oxalic acid without and with UV light. For the films anodized in 1 and 0.5 M oxalic acid the position of the emission peak for band-to-band transition are 3.18 and 3.21 eV (without UV light), respectively. With the decreasing concentration of oxalic acid (0.3 M), the crystal size decreases which in turn shifts the position of the peak of the PL spectrum into the higher energy level i.e. 3.47 eV. The same trend can be observed for the films anodized with UV light. Here the PL energy shift is observed from 3.17 eV for 1 M and from 3.19 eV for 0.5 M oxalic acid to 3.43 eV for the films anodized in 0.3 M oxalic acid. A relative decrease in the PL energy for the films grown in the presence of UV light for all the concentrations of oxalic acid studied is eventually due to crystal growth.

## 4 Discussions

When zinc sheet was dipped into the oxalic acid electrolyte and 10 V potentiostatic bias was applied, the elemental zinc in the anode converted to $Zn^{++}$ ions by releasing two electrons, which moved to the cathode. The water molecules were ionized into $H^+$ and $OH^-$ and the $OH^-$ ions were attracted towards the anode, resulting in the formation of $Zn(OH)_2$ and then to ZnO. The anodized ZnO was then etched by oxalic acid ($C_2H_2O_4$) to zinc oxalate. The etching was accelerated by UV light. The overall rate of the photoelectrochemical (PEC) oxidation and etching is determined by the photocurrent, which is proportional to the hole density at the interface between ZnO and the electrolyte.

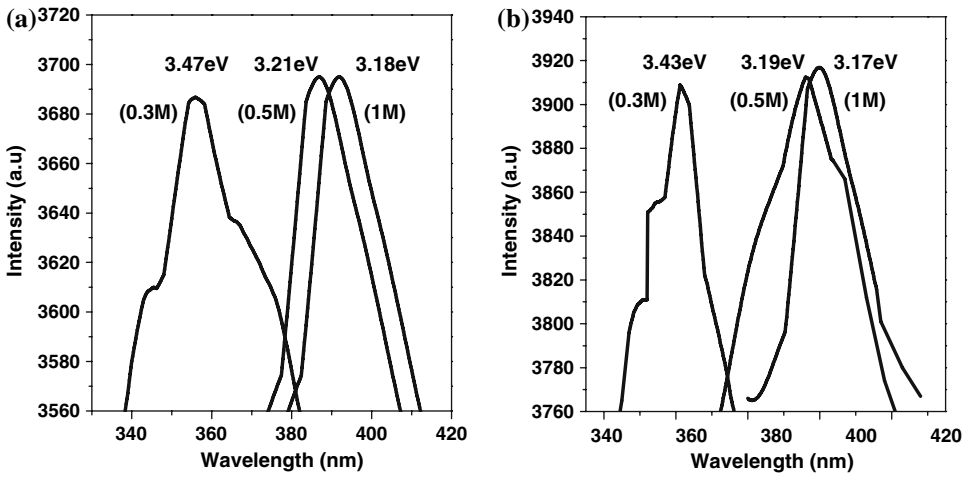


**Fig. 5** Photoluminescence of ZnO films obtained by anodization of Zn in different concentrations of oxalic acid (**a**) in absences of UV light and (**b**) in the presence of UV light. It can be observed that there is a significant blue shift at 0.3 M oxalic acid

(1) Anode reaction:

(i) Anodization

$$\begin{aligned} &Zn \rightarrow Zn^{++} + 2e^- \\ &H_2O \rightarrow H^+ + OH^- \text{ (acidic medium)} \\ &Zn^{++} + 2OH^- \rightarrow Zn(OH)_2 \\ &Zn(OH)_2 \rightarrow ZnO + H_2O \end{aligned} \quad (1)$$

(ii) Etching

$$\begin{aligned} &ZnO + C_2H_2O_4 + 2H^+ \leftrightarrow ZnC_2O_4 + H_2O \\ &OH^- + OH^- \rightarrow H_2O + O^- \\ &O^- + O^- \rightarrow O_2 \uparrow \end{aligned} \quad (2)$$

(2) Cathode reaction:

$$2H^+ + 2e^- \rightarrow H_2$$

Porous ZnO thin films can be obtained with a few defects where the etching rate is quite fast with UV illumination due to generation of more holes. We used the UV pulse of 10 min duration with an interval of 10 min. Besides the oxidation of Zn, holes also activate the etching of ZnO. Therefore, the formation and etching of ZnO continues parallelly with different kinetic rates. In order to promote the crystal growth the atoms must have sufficient activation energy to migrate along the surface until the appropriate locations are found. The optical excitation provides this enhanced activation energy to the atoms to move to the ZnO-electrolyte interface for crystal growth. Due to this reason the crystallinity of ZnO increases (Fig. 1). As the rate of anodization of Zn is enhanced with UV radiation, the peak intensity of Zn (101) decreases more and the intensity of the ZnO peaks (101) and (110) increases which are evident from Fig. 1. From the resistivity measurements it was observed that the ZnO films grown with the exposure of UV light have higher resistivity than that of the films grown without UV light. With UV exposure, the etching rate is higher compared to that without UV. As a result the thickness decreases and so the resistivity increases (Table 2). In addition, increase in pore size in the presence of UV contributes further to the increase in resistivity. The porous structures are disordered due to absence of long-range translational periodicity. As the crystal size decreases the extended localization in the conduction and valence band increases (quantum confinement effect). As a result the absorption of photon is mainly by the porous surface and by the grain boundary of the samples and the absorption edge is, therefore, blue shifted as is depicted in both the absorption spectra and PL spectra of ZnO thin films grown in different concentrations of oxalic acid (Figs. 3, 5). In fact, with lower electrolyte concentrations crystallinity decreases and a nanocrystalline phase in an amorphous surrounding creates quantum confinement [25]. In our investigation this effect is apparent with 0.3 M oxalic acid.

## 5 Conclusion

Our experiments on the electrochemical depositions and the characterizations of the nanoporous ZnO thin films demonstrated that the nanoporosity of ZnO films can be significantly controlled by the molar concentrations of the electrolyte and also by using pulsed UV light during growth. The presence of UV light during the anodization of Zn increases the growth rate as well as the etching rate of ZnO. A blue shift of the films was observed in both the optical absorption and PL spectra and it can be envisaged as due to the quantum confinement effect. Blue shift, as experimentally observed, was verified by a calculation using Brus formula and we found a reasonable agreement between the two.

## References


1. M.M. Driscoll et al., in *Proceedings IEEE International Ultrasonic Symposium*, pp. 365–369 (1986)
2. M.S. Wu, A. Azuma, T. Shiosaki, T. Kawabata, IEEE Trans. Ultrason. Ferroelectr. Freq. Control **36**, 442–445 (1989)
3. M.H. Huang et al., Science **292**, 1897 (2001)
4. G.D. Mahan, J. Appl. Phys. **54**, 7 (1983)
5. K. Keis, E. Magnusson, H. Lindstrom, S.E. Lindquist, A. Hagfeldt, Sol. Energy Mater. Sol. Cells **73**, 51 (2002)
6. D. Gruber, F. Kraus, J. Muller, Sens. Actuators **B 92**, 81 (2003)
7. S.W. Kim, S. Fujita, S. Fujita, Appl. Phys. Lett. **81**, 5036 (2002)
8. X.W. Sun, H.S. Kwok, J. Appl. Phys. **86**, 408 (1999)
9. D.K. Hwang, S.H. Kang, J.H. Lim, E.J. Yang, J.Y. Oh, J.H. Yang, S.J. Parka, Appl. Phys. Lett. **86**, 222101 (2005)
10. Z.K. Tang, G.K.L. Wong, P. Yu, M. Kawasaki, A. Ohtomo, H. Koinuma, Y. Segawa, Appl. Phys. Lett. **72**, 25 (1998)
11. P. Bhattacharyya, P.K. Basu, H. Saha, S. Basu, Sens. Lett. **4**, 371–376 (2006)
12. F.K. Shan, Y.S. Yu, J. Eur. Ceram. Soc. **24**, 1869 (2004)
13. N.K. Zayer, R. Greef, K. Rogers, A.J.C. Grellier, C.N. Pannell, Thin Sol. Films **179**, 352 (1999)
14. D. Bao, A. Kuang, H. Gu, Thin Sol. Films **37**, 312 (1998)
15. H. Ishizaki, M. Imaizumi, S. Matsuda, M. Izaki, T. Ito, Thin Sol. Films **65**, 411 (2002)
16. P.N. Bartlett, J.J. Baumberg, P.R. Birkin, M.A. Ghanem, M.C. Netti, Chem. Mater. **14**, 2199 (2002)
17. Q.B. Meng, C.H. Fu, Y. Einaga, Z.Z. Gu, A. Fujishima, O. Sato, Chem. Mater. **14**, 83 (2002)
18. H. Yan, Y. Yang, Z. Fu, B. Yang, L. Xia, S. Fu, F. Li, Electrochem. Commun. **7**, 1117 (2005)
19. G.S Wua T. Xiea, X.Y. Yuana, Y. Lia, L. Yanga, Y.H. Xiaoa, L.D. Zhanga, Solid State Commun. **134**, 485 (2005)
20. E.A. Davis, N.F. Mott, Philos. Mag. **22**, 903 (1970)
21. Z.H. Hwang, J.M. Hwang, H.L. Hwang, W.H. Hung, Appl. Phys. Lett. **84**, 19 (2004)
22. L. Brus, J. Phys. Chem. **90**, 2555 (1986)
23. Y. Kayanuma, Phys. Rev. **B 38**, 9797 (1988)
24. K.K. Kim, N. Koguchi, Y.W. Ok, T.Y. Seong, S.J. Park, Appl. Phys. Lett. **84**, 3810 (2004)
25. S.T. Tan, B.J. Chen, X.W. Sun, W.J. Fan, H.S. Kwok, X.H. Zhang, S.J. Chua, J. Appl. Phys. **98**, 013505 (2005)